

## **EXPRIMENTAL STUDIES ON AN ORGANIC RANKINE CYCLE (ORC) SYSTEM UNDER VARIABLE CONDENSATION TEMPERATURE**

Feibo Xie, Tong Zhu \*, Jihua Liu, Naiping Gao, Wei An

College of Mechanical Engineering, Tongji University,  
Siping Road 1239, Shanghai, China  
E-mail: zhu\_tong@tongji.edu.cn  
Tel: 86-21-65983867

\* Corresponding Author

### **ABSTRACT**

For a thermal power system the operating condensation temperature fluctuates significantly throughout the year in many areas due to the change of ambient temperature. Therefore, off-design operation of an Organic Rankine Cycle (ORC) system is unavoidable. The present paper focuses on the test and analysis of an ORC system using R123 as the working fluid under various condensation temperature conditions. A scroll expander was integrated into the ORC system and connected with a synchronous generator. The exhaust gas from a furnace and the water from the cooling tower were adopted to simulate the low-grade heat source and the cold source, respectively. The temperature of the exhaust gas was about 180 °C. With the increasing of the cold water temperature from 22 °C to 42 °C, the condensation temperature of the working fluid varied from 50 °C to 65 °C and the pressure from 0.21MPa to 0.32MPa, respectively. It affected the expansion ratio and the temperature difference between the inlet and outlet of the expander. The performances of the expander, evaporator, condenser and the whole system were influenced subsequently. The measured electric power output declined from 2.36kW to 1.54kW, and the thermal efficiency fell from 7.25% to 5.52% as well. Under the operation conditions, the electric power and thermal efficiency decreased, by 34.75% and 23.86%, respectively. These results indicate that the operating condensation temperature plays a key role on the performance of the ORC system, and suggest that a proper condensation temperature is important to the design and operation of the ORC system.

### **1. INTRODUCTION**

Energy crisis and global warming have greatly accelerated the development of low grade heat recovery technologies. An Organic Rankine Cycle (ORC) is regarded as a reasonable and promising way for power generation from low grade heat sources due to its high efficiency and flexibility (Tchanche B. et al., 2011; Velez F. et al., 2012; Ziviani D. et al., 2014). Compared to steam Rankine Cycles (RC), ORCs prefer organic fluids to low boiling points to improve the efficiency in low temperature applications. Several large scale ORCs have been available on the market (Quoilin S. et al., 2013; Tchanche B. et al., 2014). However, most of small-scale ORCs are still at the initial stage and receive increasingly striking attention due to its great market potential in low grade heat sources. ORCs show dramatic potential in utilization of geothermal (Gu Z. et al., 2002; Franco A. et al. 2009), solar energy (Joan B. et al., 2008; Pei G. et al., 2010), industrial waste heat (Liu B. et al., 2004; Dai Y. et al., 2009; Srinivasan K. et al., 2010; Zhou N. et al., 2013), engine exhaust gas (Invernizzi C. et al., 2007) and biomass (Martina P. et al., 2010). Over the past several decades, this wide range of applications has encouraged researchers' efforts to provide suitable ORC solutions. Thus various investigations have been carried out for working fluid selections (Hung T. et al., 2001; Saleh B. et al., 2007; Tung T. et al., 2010) and parameter optimizations (Wei D. et al., 2008; Quoilin S. et al., 2010; Quoilin S. et al., 2011; Lee Y. et al., 2012; Bracco R. et al., 2013; Minea V. et al., 2014).

Unlike RCs, ORCs, especially small scale, easily suffer the influence of off-design operation conditions. Heat sources for ORCs are usually unsteady. An industrial waste heat source usually fluctuates in a certain range because of the variation of the upstream production process. The solar radiation intensity fluctuates with the time of day and the season. The variable operation has been becoming a hotspots of ORCs studies recently. Many studies indicate that the performance and operating parameters of an ORC are sensitive to the changes in the heat source temperature (Bangbopa M. et al.,2013; Ibarra M. et al., 2014), the working fluid flow rate (Bracco R. et al.,2013;Miao Z. et al.,2015) and the load (Miao Z. et al.,2015). And variations of the entering cooling fluid temperature also have an important influence on the output power and cycle efficiency of the ORC (Lee Y. et al.,2012; Li J. et al., 2014).

Additionally the expander is a critical component of an ORC. Among positive displacement expansion machines, a scroll expander is widely regarded as a potential and promising candidate for a kW-scale ORC due to compactness, high efficiency, few movement part, broad availability and so on (Bao J. et al., 2013; Song P. et al., 2015). Generally, the scroll expander is mainly modified from a scroll compressor (Lermort V. et al.,2009; Declaye S. et al., 2013; Liu G. et al.,2015), and elaborately designed for an ORC are hardly reported.

In the present work, an ORC using an oil-free scroll expander is tested and analyzed. R123 was adopted as the working fluid. The authors focus on the steady-state expander operation characteristic and performance of the ORC system under various cooling water temperature conditions, which simulates seasonal and daily variations of the ambient temperature. Under these conditions, the key operating parameters, which mainly includes pressures and temperatures at the expander inlet and outlet, electric output power and cycle efficiency, are analyzed,.

## **2. TEST BENCH DESCRIPTION**

### **2.1 Experimental testing rig**

In this section, the brief schematic diagram of the ORC is shown in Figure 1 (a). The thermodynamics of the ORC is similar to that of the RC. The T-s diagram of the thermodynamic processes is shown in Figure 1 (b). The liquid working fluid pressurized by the working fluid pump in the evaporator absorbs the heat from the low temperature heat source and becomes the high pressure superheating vapor. The high pressure and temperature vapor expands in the scroll expander to drive the synchronous generator. The low pressure superheating vapor exhausted from the scroll expander evolves through precooling to condensing to overcooling process in the condenser and is changed into liquid, and then feeds back to the evaporator via the pump. Then this process completes a power circulation.

The major components of the ORC include an evaporator, a scroll expander, a condenser, a working fluid pump, a cooling water tower, a synchronous generator, and other auxiliary equipments. R123 was selected as the working fluid. The exhaust gas from a furnace burning flue gas was utilized to simulate a low grade heat source. A cooling water tower installed in the outdoor cooled down the cooling water from the condenser.

A tube-shell heat exchanger with the heat transfer area of 4.9 m<sup>2</sup> was used as the condenser. And here the superheated working fluid is pre-cooled, condensed and slightly sub-cooled by the cooling water.

The working fluid pump is a diaphragm metering pump and its displacement can be adjusted by its stroke, which allowed controlling the R123 flow rate through the cycle. It could provide the maximum volumetric flow rate and pressure, 800L/h and 2MPa, respectively.

A finned-tube exchanger was selected as the evaporator according to the type of the low temperature heat source, and its total heat transfer area is 14m<sup>2</sup>.

An oil-free scroll expander was used for the expansion process, which was elaborately designed for the ORC by Air Squared. Some basic parameters about the scroll expander are listed in Table 1.

An synchronous generator was driven by the scroll expander through belt- pulley coupling. The rated output power and rated rotate speed was 5kW and 1500rpm, respectively. Several bulbs was used to consume electricity from the generator.

In the test rig, the measured parameters included the pressure and temperature at inlet and outlet of four primary devices, flow rates of the working fluid and the cooling water. In addition, the detailed information of these main measurement instruments is listed in Table 2.

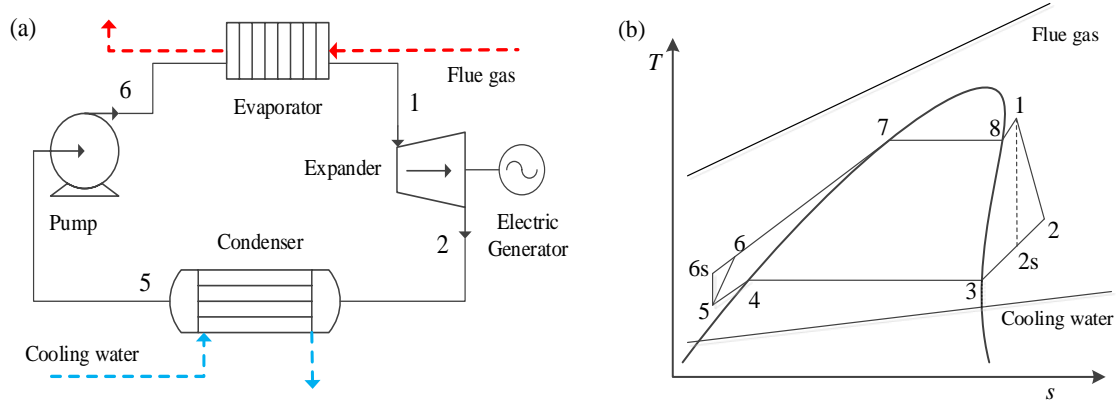


Figure 1: Schematic diagram of (a) the ORC and (b) T-s of the ORC

Table 1: Basic parameters of the scroll expander

Parameters	Unit	Value
Type	--	E22H38N4.25(oil-free)
Suction volume	cm <sup>3</sup> /r	73.6
Max. rotational speed	rpm	3600
Max. inlet pressure	MPa	1.38
Max. inlet temperature	°C	175
Built-in volume ratio	--	3.5

## 2.2 Thermodynamic analysis equations

Several different parameters were used for the analysis of the experimental data obtained under the variation of the entering cooling water temperature condition.

Table 2: Main instruments used in the test rig

Parameters	Sensors	Range	Accuracy
Temperature	K-type thermocouple	0-1580K	±0.1K
Pressure	diffused silicon pressure transmitter	0-2.5MPa	±0.2%
Liquid turbine flowmeter	LWGY-2Y	1-10m <sup>3</sup> /h	±0.1%
vortex-shedding flowmeter	BF-LUGB32246	15-150m <sup>3</sup> /h	±1.5%

The heat absorbed by the working fluid from the low temperature heat source in the evaporator is calculated by Equation (1):

$$Q_{\text{evap}} = m_{\text{wf}} (h_{\text{wf, evap, out}} - h_{\text{wf, evap, in}}) \quad (1)$$

The heat released by the working fluid towards the cooling water in the condenser is calculated by Equation (2):

$$Q_{\text{cond}} = m_{\text{wf}} (h_{\text{wf, cond, in}} - h_{\text{wf, cond, out}}) \quad (2)$$

The working fluid pump consumption is calculated by Equation (3):

$$W_p = m_{wf}(h_{wf,pump,out} - h_{wf,pump,in}) \quad (3)$$

The net electric output power in the test is calculated by Equation (4):

$$W_{net} = W_{ele} - W_p \quad (4)$$

where  $W_{ele}$  is the electric power from synchronous generator which is measured by the electro-dynamometer as the power consumed on the bulbs.

The cycle electric efficiency is defined by Equation (5):

$$\eta_{ORC} = \frac{W_{net}}{Q_{evap}} \quad (5)$$

The expander isentropic efficiency and electric isentropic efficiency, is defined by Equation (6) and (7), respectively:

$$\varepsilon_s = \frac{h_{wf,exp,in} - h_{wf,exp,out}}{h_{wf,exp,in} - h_{wf,exp,out,s}} \quad (6)$$

$$\varepsilon_{s,ele} = \frac{W_{ele}}{m_{wf}(h_{wf,exp,in} - h_{wf,exp,out,s})} \quad (7)$$

The pressure ratio of the expander, is defined by Equation (8):

$$r_p = \frac{P_{exp,in}}{P_{exp,out}} \quad (8)$$

### 2.3 Operating procedure

The ORC rig was tested under varying the cooling water inlet temperature. For this, as the ambient temperature cannot be controlled, different operating conditions had been achieved during the tests by replacing the higher temperature water in the outdoor cooling tower. On the other hand, the flue gas inlet temperature and flow rate kept steady by the flue gas flow rate and air-input amount, and the flow rate of the cooling water was imposed with a fixed frequency set point in the centrifugal water pump. In Table 3, it can be seen that the operating range obtained during the tests for each variable.

**Table 3:** The operating parameters during the tests

Parameter	Unit	Value
$t_{hf}$	°C	180
$V_{cf,cond}$	m <sup>3</sup> /h	20
$t_{cf,cond,in}$	°C	20-45
$P_{exp,in}$	MPa	0.9-1.1
$P_{exp,out}$	MPa	0.2-0.35

### 3. RESULTS AND DISCUSSION

From the experimental data obtained during the tests, an analysis has been conducted, and these results are exposed and discussed in this section.

Figure 2 shows the variation of the pressure and saturation temperature at the condenser inlet under the different cooling water temperature. The pressure was found to be approximately proportional to the entering cooling water temperature. The saturation temperature also increased linearly. This phenomenon was in accordance with the mechanism of heat transfer at the condenser. This was because when the entering cooling water temperature increase and other parameters (for example flow rates of the working fluid and cooling water), the coefficient and area of heat transfer had little effect on. The increase of the pressure at the condenser inlet inevitably results into the increase of the pressure at the expander outlet, and this could have a great effect on the expander performance.

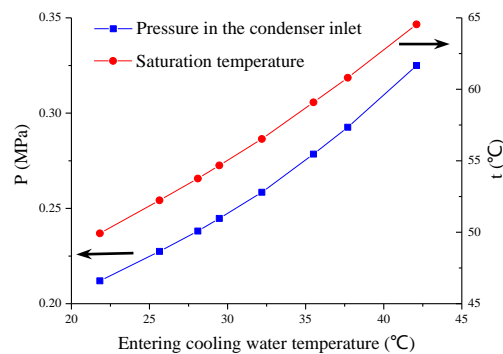
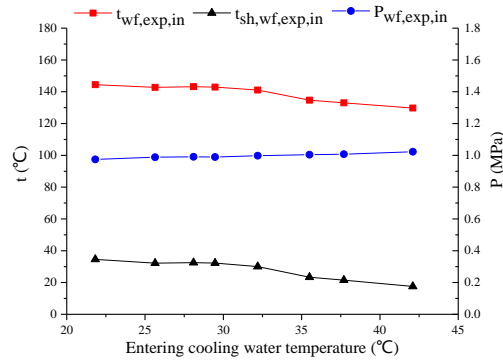


**Figure 2:** The pressure and saturation temperature at the condenser inlet vs. the entering cooling water temperature

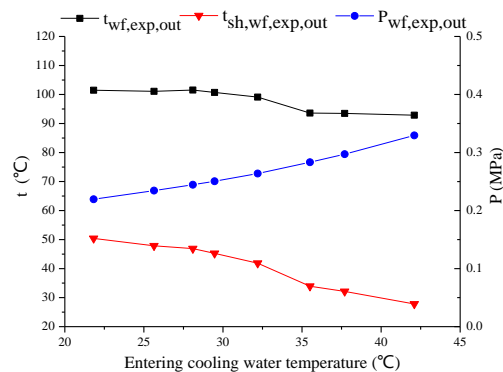
The variation of vapor pressure, temperature and superheating degree at the expander inlet are shown in the Figure 3. The vapor pressure slightly increased, and the temperature and the degree of superheating decreased with the increase of the entering cooling water temperature. This phenomenon agreed with the scroll expander characterization and the heat transfer mechanism in the evaporator. The higher scroll expander back pressure increased the discharge resistance and resulted in the higher pressure at the expander inlet. The higher vapor pressure meant the higher evaporation temperature in the evaporator. When the temperature and flow rate of the heat source at the evaporator inlet was relatively steady, it meant that the heat-transfer temperature difference decreased. The preheating and evaporating area enlarged, and the superheating area shrank. The decrease in the superheating area led to the slight decrease of the vapor temperature at the expander inlet. And this process made the superheating degree decrease.

Figure 4 shows the variation of vapor pressure, temperature and superheating degree at the expander outlet. Generally speaking, the vapor temperature at the expander outlet decreased with the entering cooling water temperature, and the vapor pressure increased. So these reduced the superheating degree. These are because the lower heat flux in the evaporator at higher entering cooling water temperature reduced the heat transfer load of the evaporator and the temperature at the expander inlet decreased. Moreover, it is obvious that the superheating degree at the expander outlet, about 50 °C is relatively high, especially under the lower entering cooling water temperature, and it could be a good choice to recover this part of heat by an internal heat exchanger (IHE). This could benefit to promote the thermal efficiency of the ORC.

The pressure ratio and temperature drop through the scroll expander were calculated and analyzed by using data from tests and is shown in Figure 5. The pressure ratio in Figure 5 is known as external pressure ratio because of the pressure sensors at the tubes connecting with the expander inlet and outlet. A higher pressure ratio through the expander leads a higher driving force for the expander. When the entering cooling water temperature increased, the relative increase of the vapor pressure at the expander outlet is larger than that at the inlet. This process results in the decrease of the pressure ratio and the pressure, and the output power could decrease.



**Figure 3:** The key operating parameters characterization at the expander inlet during the tests



**Figure 4:** The key operating parameters characterization at the expander outlet during the tests

Based on the collected operating parameters of the expander, the isentropic efficiencies is calculated and shown in Figure 6. It can be shown clearly that firstly the scroll expander isentropic efficiencies slightly descended with the increase in the entering cooling water temperature, increased dramatically, and slight decreased with the further increase in the entering cooling water temperature. The maximum isentropic efficiency was obtained when the entering cooling water temperature was 35.5 °C, and at this time the volume ratio was 3.6, which was very closed to the design value 3.5. In addition, the isentropic efficiencies calculated by Equation (6) was relative too high because the heat losses the scroll expander was not negligible during the test (Declaye S. et al., 2013). So it is hardly expected to elucidate the trends only by means of the experimental results because many factors, such as pressure losses, mechanical friction and leakage, affected the isentropic efficiency. Beside the scroll expander electric isentropic efficiency slightly decreased with the increase of the cooling water temperature, seen in Figure 6.

Figure 7 shows the variation of the measured electric power output and the cycle thermal efficiency with the increase of the entering cooling water temperature. Definitely, the electric power output and the cycle thermal efficiency decrease with the increase of the entering cooling water temperature. When the entering cooling water temperature increase from 21 °C to 42 °C, the measured electric power output declines from 2.36kW to 1.54kW, and the cycle thermal efficiency falls from 7.25% to 5.52% as well. These mean that when the entering cooling water temperature increases by 1 °C, the electric power output decreases by 1.65%. Under the operating conditions, the electric power output and thermal efficiency decreases, by 34.75% and 23.86%, respectively. It is noted that the relative decrease in the electric power output was more important than that in the thermal efficiency. The reason is likely that the heat absorbed by the working fluid from the heat source at the evaporator also decreases with the entering cooling water temperature, but the variation slowered by lower than that of the electric power output. The heat absorbed by the working fluid at the evaporator decreases because the saturation temperature in the evaporator and the enthalpy at the evaporator inlet increase.

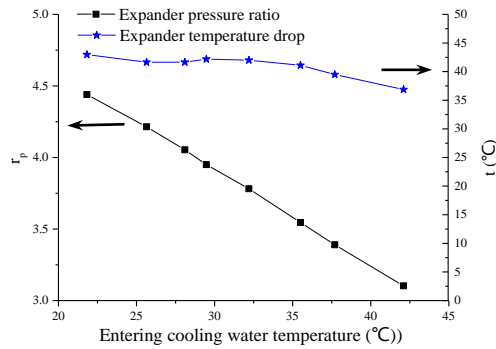


Figure 5: The pressure ratio and temperature drop through the expander during the tests

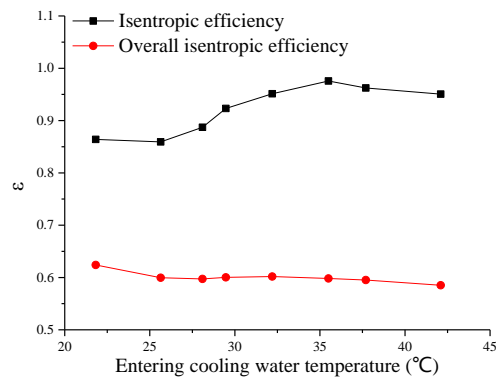


Figure 6: The isentropic efficiency characterization during the tests

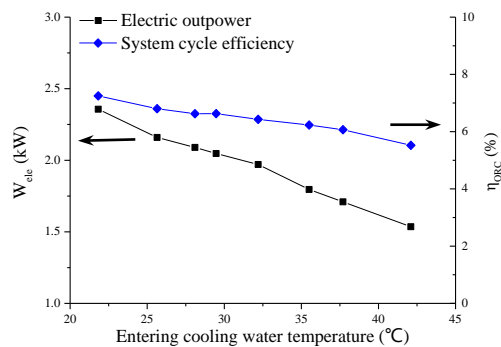


Figure 7: The ORC performance characterization during the tests

## 6. CONCLUSIONS

Focused on the exploration of kW-scale ORC system, this investigation presents the test and analysis of the operation characteristic and performance of an ORC rig with R123 as the working fluid. A oil-free scroll expander was adopted and then converted heat energy into mechanical power. Operation characteristics were compared under various cooling water temperatures from 22 °C to 42 °C, which the condensation temperature of the working fluid varied from 50 °C to 65 °C and the pressure from 0.21MPa to 0.32MPa, respectively. The measured electric power output declined from 2.36kW to 1.54kW, and the cycle thermal efficiency fell from 7.25% to 5.52% as well. Under the operation conditions, the electric output power and thermal efficiency decreased, by 34.75% and 23.86%, respectively.

For the tests, the entering cooling water temperature has a great effect on the electric output power and thermal efficiency by the variation of the pressure at the scroll expander outlet. And this means that the performance of the ORC could be sensitive to the seasonal and daily variation of the ambient temperature and suggest that a proper condensation temperature is important to the design and operation of the ORC system.

## NOMENCLATURE

$h$	enthalpy	kJ/kg
$m$	mass flow rate	kg/s
$P$	pressure	MPa
$Q$	thermal power	kW
$r_p$	pressure ratio	-
$r_v$	volume ratio	-
$s$	entropy	kJ/kg/K
$t$	temperature	°C
$V$	volume	m <sup>3</sup>
$W$	power	kW

### Greek symbols

$\varepsilon$	efficiency	%
$\eta$	efficiency	%
$\rho$	density	kg/m <sup>3</sup>

### Subscript

cf	cooling fluid
cond	condenser
ele	electric
evap	evaporator
exp	expander
hf	heat fluid
in	inlet
oc	overcooling
out	outlet
p	pump
s	isentropic
sat	saturation
sh	superheat
wf	working fluid

## REFERENCES

- Bamgbopa, M., Uzgoren, E., 2013, Numerical analysis of an organic Rankine cycle under steady and variable heat input, *Applied Energy*, vol. 107 : p. 219-228.
- Bao, J., Zhao, L., A review of working fluid and expander selections for organic Rankine cycle, *Renewable and Sustainable Energy Reviews*, vol. 24 : p. 325-342.
- Bracco, R., Clemente, S., Micheli, D., Reini, M., 2013, Experimental tests and modelization of a domestic-scale ORC (Organic Rankine Cycle), *Energy*, vol. 58 : p. 107-116.
- Dai, Y., Wang, J., Gao, L., 2009, Parametric optimization and comparative study of organic Rankine cycle (ORC) for low grade waste heat recovery, *Energy Conversion and Management*, vol. 50 : p. 576–582.
- Declaye, S., Quoilin, S., Guillaume, L., Lemort, V., 2013, Experimental study on an opendrive scroll expander integrated into an ORC (Organic Rankine Cycle) system with R245fa as working fluid, *Energy*, vol. 55 : p. 173-183.
- Franco, A., Villani, M., 2009, Optimal design of binary cycle power plants for water-dominated, medium-temperature geothermal fields, *Geothermics*, vol. 38 : p. 379–391.
- Gu, Z., Sato, H., 2002, Performance of supercritical cycles for geothermal binary design, *Energy Conversion and Management*, vol. 43 : p. 961–971.



- Hung, T., 2001, Waste heat recovery of organic Rankine cycle using dry fluids, *Energy Conversion and Management*, vol. 42 : p. 539-553.
- Ibarra, M. Rovira, A., Alarcon-Padilla, D., Blanco, J., 2014, Performance of a 5kWe Organic Rankine Cycle at part-load operation, *Applied Energy*, vol. 120 : p. 147-158.
- Invernizzi, C., Iora, P., Silva, P., 2007, Bottoming micro-Rankine cycles for micro-gas turbines, *Applied Thermal Engineering*, vol. 27 : p. 100–110.
- Joan, B., Jesús, L., Eduardo, L., Silvia, R., Alberto, C., 2008, Modelling and optimisation of solar organic Rankine cycle engines for reverse osmosis desalination, *Applied Thermal Engineering*, vol. 28 : p. 2212–2226.
- Lee, Y., Kuo, C., Wang, C., 2012, Transient response of a 50 kW organic Rankine cycle system, *Energy*, vol. 48 : p. 532-538.
- Lemort, V., Quoilin, S., Cuevas, C., Lebrun, J., 2009, Testing and modeling a scroll expander integrated into an organic Rankine cycle, *Applied Thermal Engineering*, vol. 29 : p. 309-3102.
- Li, J., Pei, G., Ji, J., Bai, X., Li, P., Xia, L., 2014, Design of the ORC (organic Rankine cycle) condensation temperature with respect to the expander characteristics for domestic CHP (combined heat and power) applications, *Energy*, vol. 77 : p. 579-590.
- Liu, B., Chien, K., Wang, C., Effect of working fluids on organic Rankine cycle for waste heat recovery, *Energy*, vol. 29 : p. 1207–1217.
- Liu, G B., Zhao, Y., Yang, Q., Wang, L., Tang, B., Li, L., 2015, Theoretical and experimental research on scroll expander used in small-scale organic Rankine cycle system, *Journal of Process Mechanical Engineering*, vol. 229 : p. 25-35.
- Martina, P., Shane, W., Philip, O., 2010, Evaluation of energy efficiency of various biogas production and utilization pathways, *Applied Energy*, vol. 87 : p. 3305–3321.
- Miao, Z., Xu, J., Yang, X., Zou, J., 2015, Operation and performance of a low temperature organic Rankine cycle, *Applied Thermal Engineering*, vol. 75 : p. 1065-1075.
- Pei, G., Li, J., Ji, J., 2010, nalysis of low temperature solar thermal electric generation using regenerative organic Rankine cycle, *Applied Thermal Engineering*, vol. 30 : p. 998–1004.
- Quoilin, S., Aumann, R., Grill, A., Schuster, A., Lemort, V., Spliethoff, H., 2011, Dynamic modeling and optimal control strategy of waste heat recovery Organic Rankine Cycles, *Applied Energy*, vol. 88 : p. 2183-2190.
- Quoilin, S., Broek, M., Declaye, S., Dewallef, P., Lemort, V., 2013, Techno-economic survey of Organic Rankine Cycle (ORC) systems, *Renewable and Sustainable Energy Reviews*, 2013, vol. 22 : p. 168-186.
- Quoilin, S., Lemort, V., Lebrun, J., 2010, Experimental study and modeling of an organic Rankine cycle using scroll expander, *Applied Energy*, vol. 87 : p. 1260-1268.
- Saleh, B., Koglbauer, G., Wendland, M., Fischer, J., 2007, Working fluids for lowtemperature organic Rankine cycles, *Energy*, vol. 32 : p. 1210-1221.
- Song, P., Wei, M., Shi, L., Danish, S., Ma, C., 2015, A review of scroll expanders for organic Rankine cycle systems, *Applied Thermal Engineering*, vol. 75 : p. 54-64.
- Srinivasan, K., Mago, P., Krishnan, S., 2010, Analysis of exhaust waste heat recovery from a dual fuel low temperature combustion engine using an organic Rankine cycle, *Energy*, vol. 35 : p. 2387-2399.
- Tchanche, B., Lambrinos, Gr., Frangoudakis, A., Papadakis, G., 2011, Low-grade heat conversion into power using organic Rankine cycles – A review of various applications, *Renewable and Sustainable Energy Reviews*, vol. 15 : p. 3963-3979.
- Tchanche, B., Petrissans, M., Papadakis, G., 2014, Heat resource and organic Rankine cycle machine, *Renewable and Sustainable Energy Reviews*, vol. 39 : p. 1185-1199.
- Tung, T., Wang, S., Kuo, C., Pei, B., Tsai, K., 2010, A study of organic working fluids on system efficiency of an ORC using low-grade energy sources, *Energy*, vol. 35 : p. 1403-1411.
- Vasile, M., 2014, Power generation with ORC machines using low-grade waste heat or renewable energy, *Applied Thermal Engineering*, vol. 69 : p. 143-154.

- Velez, F., Segovia, J., Martin, C., Antolin G., Chejne F., Quijano,A., 2012, A technical, economical and market review of organic Rankine cycles for the conversion of low-grade heat for power generation, *Renewable and Sustainable Energy Reviews*, vol. 16 : p. 4175-4189.
- Wei, D., Lu, X., Lu, Z., Gu, J., 2008, Dynamic modeling and simulation of an Organic Rankine Cycle (ORC) system for waste heat recovery, *Applied Thermal Engineering*, vol. 28 : p. 1216-1224.
- Zhou, N., Wang, X., Chen, Z., Wang, Z., 2013, Experimental study on Organic Rankine Cycle for waste heat recovery from low-temperature flue gas, *Energy*, vol. 55 : p. 216-225.
- Ziviani, D., Beyene, A., Venturini, M., 2014, Advances and challenges in ORC systems modeling for low grade thermal energy recovery, *Applied Energy*, vol. 121: p. 79-95.

#### **ACKNOWLEDGEMENT**

The authors want to acknowledge the financial support by National Fundamental Research Program 973 project (2014CB249201) "Research on the stability of complex energy system integrated natural gas and renewable energy" and ENN-Tongji Institute for Advanced Clean Energy under the project "Research on the key technologies in power generation from low-grade waste heat".